

Analytical Formulation of a Maximum Torque per Ampere (MTPA) Technique for SynRMs Considering the Magnetic Saturation

Angelo Accetta, MEMBER, IEEE
National Research Council of Italy
(CNR),
Institute for Marine Engineering (INM)
Palermo, Italy
angelo.accetta@cnr.it

Maurizio Cirrincione, SENIOR MEMBER,
IEEE
University of the South Pacific,
School of Engineering,
Laulala Campus, Suva, Fiji
m.cirrincione@ieee.org

Maria Carmela Di Piazza, SENIOR
MEMBER, IEEE
National Research Council of Italy
(CNR),
Institute for Marine Engineering (INM)
Palermo, Italy
mariacarmela.dipiazza@cnr.it

Giuseppe La Tona, MEMBER, IEEE
National Research Council of Italy
(CNR),
Institute for Marine Engineering (INM)
Palermo, Italy
giuseppe.latona@cnr.it

Massimiliano Luna, MEMBER, IEEE
National Research Council of Italy
(CNR),
Institute for Marine Engineering (INM)
Palermo, Italy
massimiliano.luna@cnr.it

Marcello Pucci, SENIOR MEMBER, IEEE
National Research Council of Italy
(CNR),
Institute for Marine Engineering (INM)
Palermo, Italy
marcello.pucci@cnr.it

Abstract— This paper proposes an analytical formulation of a maximum torque per ampere (MTPA) technique, accounting for the magnetic saturation of the iron core, specifically developed for Synchronous Reluctance Motors (SynRMs). The proposed MTPA is based on a magnetic saturation model of the SynRM, which has been obtained after simplifying a more complete magnetic model, including also cross saturation effects. This simplified magnetic model, and consequently the proposed MTPA, can be easily parameterized directly starting from a unique set of tests for the off-line identification of the motor, without the need for any complex, time consuming, and cumbersome finite element analysis (FEA) of the machine under test. The proposed MTPA has been tested experimentally on a suitably developed test set-up. Results obtained with the proposed MTPA have been compared experimentally with both the classic MTPA and the real MTPA. Results clearly show that the proposed technique permits a significant increase of the torque per ampere (TPA) with respect to the case of the classic MTPA, which does not consider magnetic saturation. TPA increase varies from 5% at 3 Nm load to 18% at 12 Nm load. Moreover, the loss of maximum torque, with respect to the real MTPA, obtained at the maximum speed and load torque with the proposed MTPA is about 15%, whereas the loss of maximum torque obtained with the classic MTPA is about 38.5%.

Keywords—Synchronous Reluctance Motor (SynRM), Maximum Torque Per Ampere (MTPA), Rotor Oriented Control

I. INTRODUCTION

Even if the first synchronous reluctance motor (SynRM) prototypes have been developed around 1923, their low performance (in terms of output torque and power) combined with their relatively high price have limited their adoption for a long time. However, their recent development has resulted in a much more reliable and robust construction. In particular, advanced rotor design has permitted increased values of the saliency ratios (9-12), to which the performance of SynRMs is strictly related [1]. Even if modern SynRMs present output power levels comparable to those of the corresponding induction motors (IM), very few companies in the world produce them. Indeed, SynRMs manufactured with high

saliency ratios are particularly suited for high performance applications, like machine tools drives, robotics, and electrical vehicles. High dynamic performance can be achieved by adopting vector control techniques and several rotor-oriented or stator flux-oriented control schemes have been developed [2]-[4]. The theoretical performance of the SynRMs is limited, however, by the strong non-linearity of the machine, particularly for its magnetic characteristics; actually, the saturation phenomena are different on the direct and quadrature axes, and significant cross-saturation phenomena are observable [5][6]. In order to minimize the effects of joule losses in the stator windings and thus optimize the electromechanical torque production, maximum torque per ampere (MTPA) techniques have been developed. MTPAs, however, do not always imply the best energy efficiency of SynRMs to be achieved, since iron losses are not included in MTPA formulation. If the magnetic circuit of the SynRM is considered linear (constant inductances), the MTPA problem leads to the classic solution, where the stator current angle δ must be kept equal to $\pi/4$ or, equivalently, the direct and quadrature components of the stator current in the rotor-oriented reference frame must be such that $i_{sx} = |i_{sy}|$ [1]. A way to deal with the magnetic saturation and iron core losses has been proposed in [7], where a set of curves have been obtained by experimental tests, providing the relationship between the stator current amplitude and the direct component of the stator current, for several values of the load torque. Afterwards, a quadratic function between the direct component of the stator current and the load torque has been deduced, by interpolating the points of minimum current amplitude. Also [8] and [9] propose MTPA techniques based on the classic relationship $i_{sx} = |i_{sy}|$. The main difference is that, while [9] proposes a classic rotor-oriented vector control and expresses the i_{sx} reference as a function of the load torque, [8] proposes a stator flux-oriented control. As a consequence, in [8], the i_{sx} and i_{sy} current components must be properly vector rotated into the stator flux reference frame. None of the two approaches, however, considers the magnetic saturation in the MTPA formulation. An approach fully

accounting for the magnetic saturation has been proposed by [10], where an algebraic magnetic model is firstly deduced based on current versus flux functions. Afterwards, the *MTPA* problem is solved numerically by adopting the *Brent* algorithm after inverting numerically the magnetic model by the *Powell* dogleg algorithm. Alternative approaches for the optimal torque control are based on specific finite element analyses (*FEA*) of the machine under test [11], requiring however precise knowledge of the machine design and construction. This paper presents, as an original contribution, an analytical formulation of an *MTPA* technique considering the magnetic saturation of the iron core and specifically developed for *SynRMs*. This technique is based on a simplified magnetic saturation model of the *SynRM*, derived by a previously developed complete magnetic model including both self and cross-saturation effects [12]. The parameterization of the simplified magnetic model, and consequently of the proposed *MTPA*, can be therefore easily developed from a unique set of few experimental tests for the off-line identification of the motor. The advantage of the proposed approach is that it can be immediately implemented in analytical form after the machine has been identified [12], without the need of either any long experimental test [8] or any involved, time consuming, and cumbersome *FEA* of the machine under test [11] or numerical optimization algorithm and function inversion [10]. The proposed *MTPA* has been tested experimentally on a suitably developed test set-up. Experimental results achieved with the proposed *MTPA* have been compared firstly with those achievable with the classic *MTPA* ($i_{sx} = |i_{sy}|$) and secondly with those achievable with the real *MTPA*, with aim of highlighting the advantages in terms, from one side, of the of torque increase capability with respect to the classic *MTPA* and, from another side, the limited torque loss with respect to the real *MTPA*. This paper is an improvement and extension of [13].

II. COMPLETE MAGNETIC MODEL OF THE SYNRM

A novel complete magnetic model of the *SynRM* has been proposed in [12], where specific original flux versus current functions have been deduced, permitting both the self and cross-saturation effects to be accounted for. In the following, this model is briefly described. For the detailed version of the model, the reader can refer to [12].

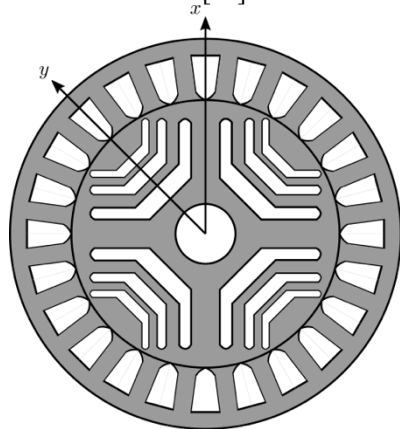


Fig. 1. Cross section of the *SynRM* with the related direct (x) and quadrature (y) axis

As for the adopted notation of the axis, Fig. 1 shows the cross section of a typical *SynRM*, where the direct (x) and quadrature (y) axis are clearly highlighted. If ψ_{sx} , ψ_{sy} are the stator direct (x) and quadrature (y) flux components in the rotor reference frame, and i_{sx} , i_{sy} are the corresponding stator current components, the flux versus current functions can be written as:

$$\begin{aligned} \psi_{sx}(i_{sx}, i_{sy}) &= \alpha(1 - e^{-ai_{sx}}) + \beta i_{sx} - \gamma \frac{(1 - e^{-bi_{sx}i_{sy}})}{i_{sx}}, \\ \psi_{sy}(i_{sx}, i_{sy}) &= \delta(1 - e^{-ci_{sy}}) + \varepsilon i_{sy} - \gamma \frac{(1 - e^{-bi_{sx}i_{sy}})}{i_{sy}} \end{aligned} \quad (1 \text{ a, b})$$

The entire magnetic behavior of the machine can be, therefore, described by functions requiring the knowledge of 8 model parameters. In [12] it has been further shown that the functions (1 a, b) properly satisfy the reciprocity conditions as for the cross-saturation, ensuring that the non-linear inductances do not generate or dissipate energy. Moreover, an identification technique of the saturation model based on stand-still tests, without the need for locking the rotor, has been proposed and validated experimentally. This identification technique exploits *Genetic Algorithms (GA)*. Starting from the flux equations in (1 a, b), the stator static inductances can be deduced as follows:

$$\begin{aligned} L_{sxx}(i_{sx}, i_{sy}) &= \frac{\psi_{sx}}{i_{sx}} = \alpha \frac{(1 - e^{-ai_{sx}})}{i_{sx}} - \gamma \frac{(1 - e^{-bi_{sx}i_{sy}})}{i_{sx}^2} + \beta, \\ L_{syy}(i_{sx}, i_{sy}) &= \frac{\psi_{sy}}{i_{sy}} = \delta \frac{(1 - e^{-ci_{sy}})}{i_{sy}} - \gamma \frac{(1 - e^{-bi_{sx}i_{sy}})}{i_{sy}^2} + \varepsilon \end{aligned} \quad (2 \text{ a, b})$$

It can be further noticed that the coefficients α , β (x axis) and δ , ε (y axis) can be physically interpreted. For example, as for the x axis, considering that $\lim_{i_{sx} \rightarrow 0} L_{sxx} = \alpha\alpha + \beta$ (since no cross-saturation occurs for $i_{sy}=0$), and $\lim_{i_{sx} \rightarrow \infty} L_{sxx} = \beta$, β can be interpreted as the self-inductance when the machine is fully saturated, and the relation $\alpha\alpha + \beta$ as the tangent of the magnetizing curve at the origin, which represents the initial state of magnetization of the iron core.

III. PROPOSED MAXIMUM TORQUE PER AMPERE (MTPA) TECHNIQUE

Eqs. (1) and (2) cannot be exploited to develop an analytical formulation of the *MTPA*, because of their strong complexity and non-linearity. To get around this problem, some simplifications have been made to the above described model, permitting the *MTPA* problem to be solved analytically. The first simplification is to neglect the cross-saturation effect, since its weight is much lower than that of the main saturation, as well known in the scientific literature. The second simplification is to neglect the saturation on the quadrature y axis. Such an assumption is reasonable since the magnetic circuit on the y axis lies mostly in air. Moreover, in [12] it is shown that the corresponding magnetic characteristic is almost linear in a wide range of i_{sy} . This implies considering a constant value of the static inductance of the y axis, $L_{syy} = L_{syy0}$. Finally, starting from (2 a), a linear variation of the static inductance L_{sxx} with the direct component of the current i_{sx} has been assumed, resulting in a quadratic dependence of the stator flux ψ_{sx} on i_{sx} , as follows:

$$L_{sxx}(i_{sx}) = \frac{\psi_{sx}}{i_{sx}} = L_{sx0} - \delta_L i_{sx}, \quad (3, 4)$$

$$\psi_{sx}(i_{sx}) = L_{sx0} i_{sx} - \delta_L i_{sx}^2$$

The three coefficients of the simplified model L_{sx0} , L_{sy0} , and δ_L can be easily deduced from the model (2), whose identification procedure is described in [12]. In particular, $L_{sxx} = a\alpha + \beta$ ($L_{syy} = c\delta + \varepsilon$) corresponds to the inductance on the x (y) axis with no excitation current $i_{sx} = 0$ ($i_{sy} = 0$), whereas δ_L can easily be retrieved on the basis of the knowledge of a single value of the inductance (2 a) L_{sxx1} , obtained for a specific value of the current i_{sx1} in deep saturation, as $\delta_L = \frac{L_{sxx0} - L_{sxx1}}{i_{sx1}}$. Fig. 2 shows the $\psi_{sx}(i_{sx})$ and $L_{sxx}(i_{sx})$ curves for the *SynRM* under test, where the magnetic saturation is considered in three ways. The black trace is related to the model described by (1 a) and (2 a), thus properly considering magnetic saturation. The blue trace is related to the linear model (flux linearly increasing with the current and constant inductance), thus not considering at all the magnetic saturation. Finally, the red trace is related to the adopted simplified model (flux increasing with the current with a quadratic dependence, and inductance linearly decreasing with the current), so that the magnetic saturation is considered even if with slight simplifications.

Starting from eq. (3), the expression of the magnetic saliency ΔL_s can be deduced, and the corresponding expression of the electromagnetic torque t_e can be obtained.

$$\Delta L_s = L_{sxx} - L_{syy} = L_{sx0} - L_{sy0} - \delta_L i_{sx} = \Delta L_{s0} - \delta_L i_{sx},$$

$$t_e = \frac{3}{2} p \Delta L_s i_{sx} i_{sy} = \frac{3}{2} p (\Delta L_{s0} - \delta_L i_{sx}) i_{sx} i_{sy} \quad (5, 6)$$

Once the model has been defined, the *MTPA* problem can be formulated as the problem of minimizing the amplitude of the stator current space-vector $|\mathbf{I}_s| = \sqrt{i_{sx}^2 + i_{sy}^2}$, subject to the constraint that the electromagnetic torque t_e must be equal to the load torque t_L . If the *Lagrangian* multiplier λ is adopted, the following function f is to be minimized.

$$f = \sqrt{i_{sx}^2 + i_{sy}^2} + \lambda(t_L - t_e) \quad (7)$$

To this aim, the following three derivatives must be computed and put equal to zero.

$$\frac{df}{di_{sx}} = \frac{i_{sx}}{\sqrt{i_{sx}^2 + i_{sy}^2}} - \lambda \left(\frac{3}{2} p \Delta L_{s0} i_{sy} - 3p \delta_L i_{sx} i_{sy} \right) = 0,$$

$$\frac{df}{di_{sy}} = \frac{i_{sy}}{\sqrt{i_{sx}^2 + i_{sy}^2}} - \lambda \left(\frac{3}{2} p \Delta L_{s0} i_{sx} - \frac{3}{2} p \delta_L i_{sx}^2 \right) = 0,$$

$$\frac{df}{d\lambda} = (t_L - t_e) = 0 \quad (8 \text{ a,b,c})$$

It can be easily demonstrated through algebraic manipulation of (8 a) and (8 b) that the following relationship between i_{sx} and i_{sy} can be found:

$$i_{sx}^3 - \frac{\Delta L_{s0}}{\delta_L} i_{sx}^2 - 2i_{sy}^2 i_{sx} + \frac{\Delta L_{s0}}{\delta_L} i_{sy}^2 = 0 \quad (9)$$

Solving the *MTPA* problem corresponds to solving the 3rd order equation (9) in i_{sx} , which corresponds to finding the direct function $i_{sx} = g(i_{sy})$ that solves (7). Eq.(3) has the following three real solutions, if $i_{sy} \neq 0$:

$$i_{sx1} = 2^{\frac{1}{3}} \sqrt[3]{\frac{2}{3} i_{sy}^2 + \frac{1}{9} \frac{\Delta L_{s0}^2}{\delta_L^2} \cos \frac{\theta}{3} + \frac{\Delta L_{s0}}{3\delta_L}},$$

$$i_{sx2} = 2^{\frac{1}{3}} \sqrt[3]{\frac{2}{3} i_{sy}^2 + \frac{1}{9} \frac{\Delta L_{s0}^2}{\delta_L^2} \cos \frac{\theta}{3} + \frac{\Delta L_{s0}}{3\delta_L}} - \sqrt[3]{2i_{sy}^2 + \frac{1}{3} \frac{\Delta L_{s0}^2}{\delta_L^2} \sin \frac{\theta}{3}},$$

$$i_{sx3} = 2^{\frac{1}{3}} \sqrt[3]{\frac{2}{3} i_{sy}^2 + \frac{1}{9} \frac{\Delta L_{s0}^2}{\delta_L^2} \cos \frac{\theta}{3} + \frac{\Delta L_{s0}}{3\delta_L}} + \sqrt[3]{2i_{sy}^2 + \frac{1}{3} \frac{\Delta L_{s0}^2}{\delta_L^2} \sin \frac{\theta}{3}} \quad (10 \text{ a, b, c})$$

Where:

$$t\theta = \frac{\frac{4}{9} i_{sy}^6 + \frac{7}{36} \frac{\Delta L_{s0}^2}{\delta_L^2} i_{sy}^4 + \frac{1}{81} \frac{\Delta L_{s0}^4}{\delta_L^4} i_{sy}^2 + \frac{8}{729} \frac{\Delta L_{s0}^6}{\delta_L^6}}{-\frac{1}{6} \frac{\Delta L_{s0}}{\delta_L} i_{sy}^2 + \frac{1}{27} \frac{\Delta L_{s0}^3}{\delta_L^3}} \quad (11)$$

If $i_{sy} = 0$, the equation gives the roots $i_{sx} = 0$ with multiplicity 2 and $i_{sx} = \frac{\Delta L_{s0}}{\delta_L}$. Obviously only the null result has physical meaning. Moreover, by applying the *Routh* criterion to equation (9) it is easy to prove that there are always 2 nonnegative real roots. Among these 3 solutions, only one corresponds to the minimum of (7). Fig. 3 shows the obtained function $i_{sx} = g(i_{sy})$ solving the *MTPA* problem in comparison with the solving function obtained in the classic *MTPA*. The latter is based on the assumption of linear magnetic characteristic, and its solution leads to the relationship $i_{sx} = |i_{sy}|$, i.e., $\delta = \pi/4$ [1].

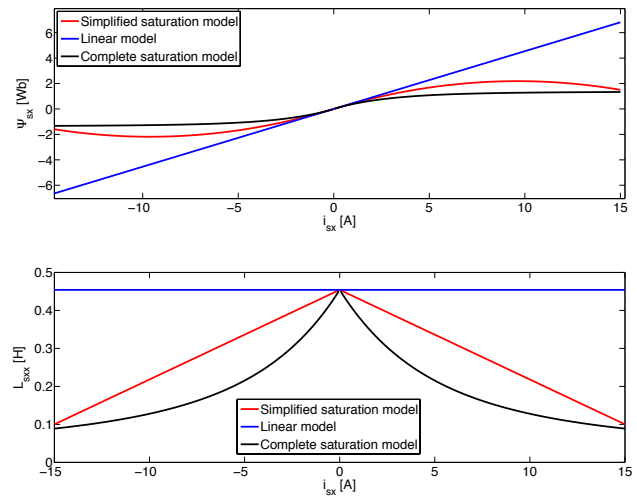


Fig. 2. $\psi_{sx}(i_{sx})$ and $L_{sxx}(i_{sx})$ curves for the *SynRM* under test

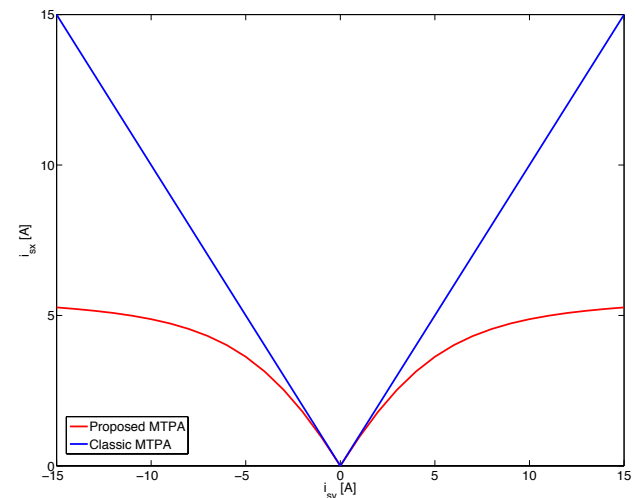


Fig. 3. $i_{sx} = g(i_{sy})$ solving the *MTPA* problem

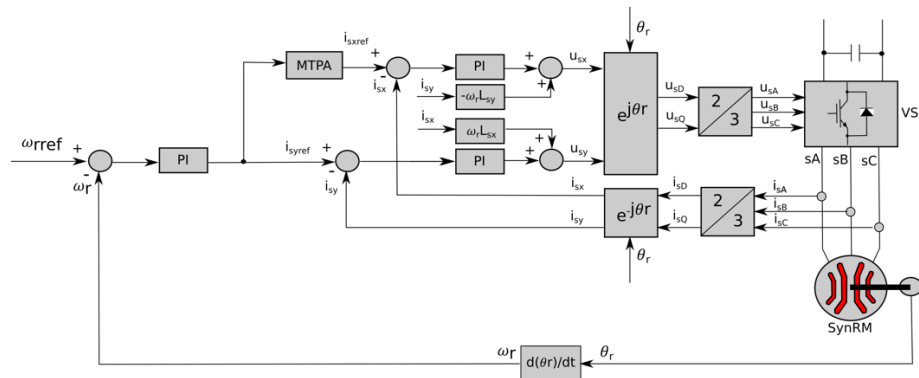


Fig. 4. Block diagram of the rotor-oriented control of the *SynRM*

It can be observed that, because of the saturation of the iron core, with the proposed *MTPA* the i_{sx} increases with i_{sy} linearly for low values of the load like the classic one, but presents a lower rate of change for increasing values of the load, finally showing a saturation phenomenon for very high values of the load. Such a behavior is physically explainable with the reduction of the L_{sxx} for increasing i_{sx} , resulting in a slower increase of the magnetizing current for increasing loads to minimize the current amplitude so that the load constraint in (7) can be met. This phenomenon can be explained also from a geometrical point of view, considering that the constant torque curve shape changes from a hyperbola (valid when the magnetic saturation is neglected) to a more complex curve because of saturation (see Fig. 7). The proposed *MTPA* belongs to model based category. The $i_{sx} = g(i_{sy})$ function relies on the knowledge of some machine parameters, particularly the difference between the stator inductances on the direct and quadrature axis (ΔL_{s0}) at zero stator current, and the rate of change of the stator inductance on the direct axis with the corresponding stator current component (δ_L). These two parameters could present a limited variation with the *SynRM* operating condition, presenting a potential limited variation with the iron losses of the machine (thus with the speed of the machine, particularly in high speed machines). Such an effect has not been considered, however, in this work and could be a further improvement of it.

IV. TEST SET-UP

The employed test set-up consists of a *SynRM* motor model *ABB 3GAL092543-BSB*. Tab. I shows the rated data of the *SynRM* under test, while Tab. II shows the parameters of the complete saturation model, identified with the technique proposed in [12], as well as the parameters of the simplified saturation model adopted in the *MTPA*. The *SynRM* is supplied by a Voltage Source Inverter (VSI) with insulated gate bipolar transistor (IGBT) modules, model *Semikron SMK 50 GB 123*, driven by a space-vector Pulse Width Modulation technique (*SV-PWM*) with PWM frequency set to 5 kHz. The *SynRM* drive has been controlled adopting a rotor oriented control [1]-[4]. Fig. 4 shows the block diagram of the adopted rotor-oriented control scheme, including the proposed *MTPA*. The proposed *MTPA* technique has been embedded in such a control scheme. Both the adopted PWM and control techniques have been implemented on a dSPACE card

(DS1103) with a PowerPC 604e at 400 MHz and a floating-point DSP TMS320F240. The sampling time of the control system has been set equal to 10 kHz. The *SynRM* motor is mechanically coupled to a torque controlled permanent magnet synchronous motor (*PMSM*) drive working as active load. Fig. 5 shows the photo of the *SynRM* drive test set-up.

TABLE I. RATED DATA OF THE ABB SYNRM

Rated Power (kW)	2.2
Rated Voltage (V)	380
Rated Frequency (Hz)	50
Pole-pairs	2
Rated speed (rpm)	1500
Rated Current (A) RMS	5.5
Rated torque (Nm)	14

TABLE II. PARAMETERS OF THE COMPLETE AND SIMPLIFIED *SynRM* SATURATION MODELS

	<i>Complete Saturation Model</i>		<i>Simplified Saturation Model</i>
a	0.35	L_{sx0}	0.4542
b	4.04	L_{sy0}	0.1882
c	1.20	δ_L	0.0236
α	0.35		
β	0.0047		
γ	0.0018		
δ	0.13		
ϵ	0.0250		

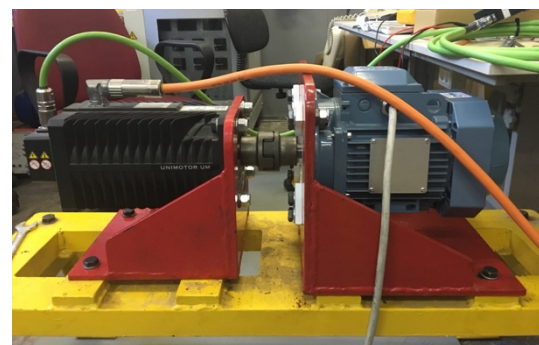


Fig. 5. Photograph of the Experimental Set-up

V. EXPERIMENTAL RESULTS

The proposed *MTPA* has been tested experimentally in the test set-up described in section IV. Results obtained with the

proposed *MTPA* have been experimentally compared, from one side with the classic *MTPA* technique, and from another side with the real *MTPA*. Two kind of tests have been performed. The first one is a dynamic test in which the *SynRM* drive is run at constant speed and a set of incremental torque steps have been applied. As for this test, the results obtained with the proposed *MTPA* have been compared with those achieved with the classic *MTPA*, in order to highlight any difference arising from the adoption of the two *MTPA* techniques, if present, in the dynamic performance of the *SynRM* drive. The second test shows the experimental steady-state electromagnetic torque that can be produced by the *SynRM* drive in the entire working range of the stator current amplitude and rotor speed. As for this test, results the results obtained with the proposed *MTPA* have been compared with those achieved with both the classic *MTPA* and the real *MTPA*. From this point of view, the adopted methodology for obtaining the steady-state real *MTPA* has been described.

A. Test 1: dynamic test

The reference speed of the drive has been set to the constant value equal to 50 rad/s. Starting from the no-load condition, a set of incremental load torque steps has been applied, equal respectively to 3, 6, 9, and 12 Nm. Fig. 6 a, b show the direct and quadrature components of the stator currents, i_{sx} and i_{sy} , obtained during this test with the classic *MTPA* (blue trace) and with the proposed *MTPA* (red trace). It can be observed that the control system works properly with both *MTPAs*, as expected. At each increase of the load torque, an increase of i_{sy} occurs and correspondingly an increase of i_{sx} , and vice versa when load decreases. It can be noted that, in accordance with Fig. 3, the increase of i_{sx} with i_{sy} is slower with the proposed *MTPA* than with the classic one. This is confirmed by Fig. 7, showing superimposed on the same graph the set of circles defining the loci at constant stator current amplitude (circles), the set of curves defining the loci at constant electromagnetic torque (different depending on the adopted *MTPA*), and finally the instantaneous trajectories obtained during the test with the proposed *MTPA* (red trace), the classic *MTPA* (blue trace) and the real *MTPA* (green trace). It can be noted that the loci at constant electromagnetic torque, which are hyperbolas in case of neglectation of the saturation of the iron core, if the proposed simplified saturation model described by (3) and (4) is adopted, become more complex curves, according to (6). It can be further noticed that the trajectory of the stator current space-vector obtained with the proposed *MTPA* lays instantaneously on the points where the constant torque curves are tangent to the constant current circles, confirming the correctness of the *MTPA*. This is not the case for the trajectory of the stator current obtained with the classic *MTPA*, laying on the bisector of the plane, as expected. It can be noted that, if the classic *MTPA* is adopted, i_{sx} increases linearly with i_{sy} , as expected, lying its trajectory on the bisector between the direct and quadrature axis. If the proposed *MTPA* is adopted, the rate of change of i_{sx} with i_{sy} is lower than in the classic *MTPA* case and a saturation of i_{sx} is observable for very high values of i_{sy} .

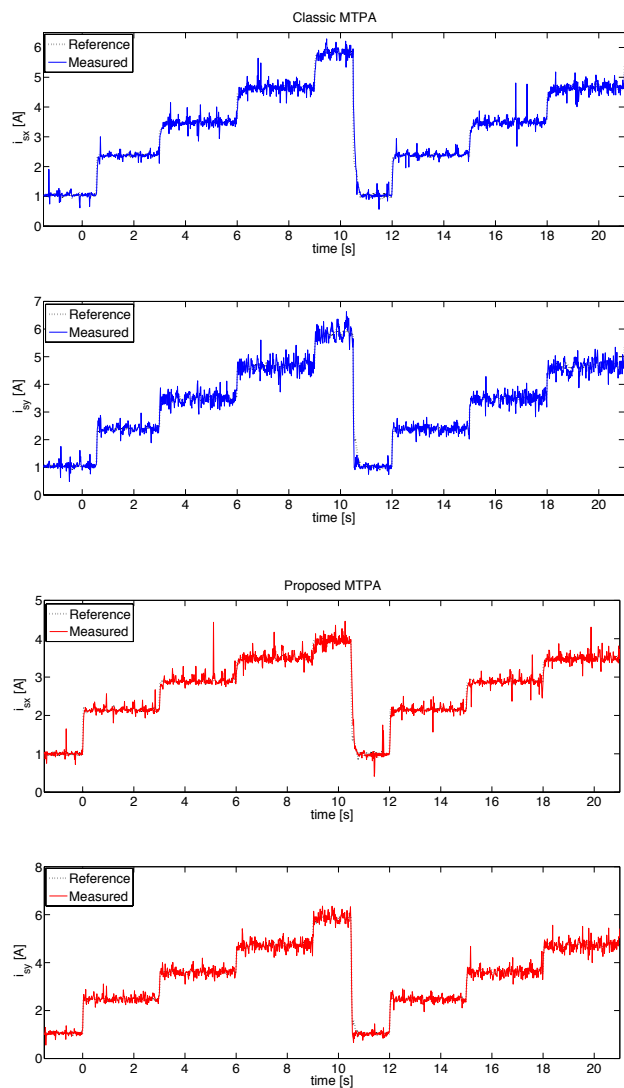


Fig. 6. a, b, direct and quadrature components of the stator current with the classic *MTPA* (a up) and with the proposed *MTPA* (b down)

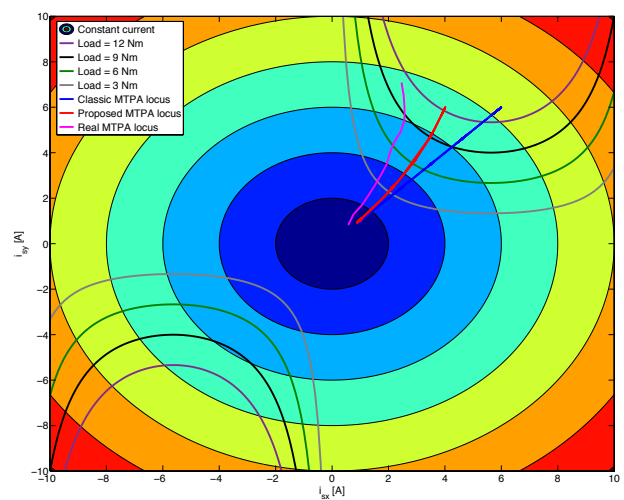


Fig. 7. Constant amplitude stator current circles, constant torque curves and $i_{sx} = g(i_{sy})$ *MTPA* loci

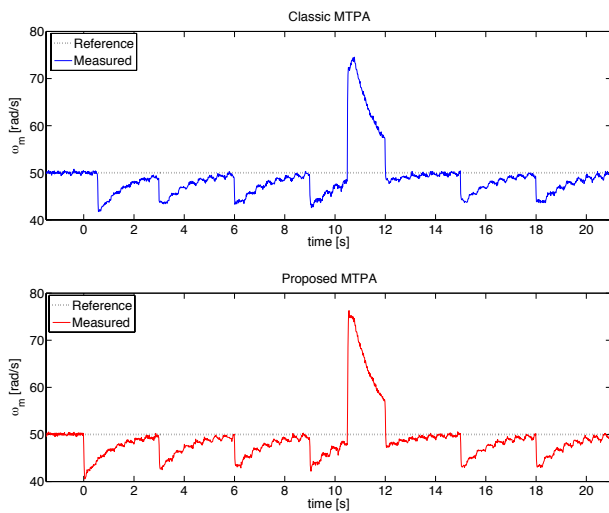


Fig. 8. Reference and measured speed with the classic and the proposed *MTPA*

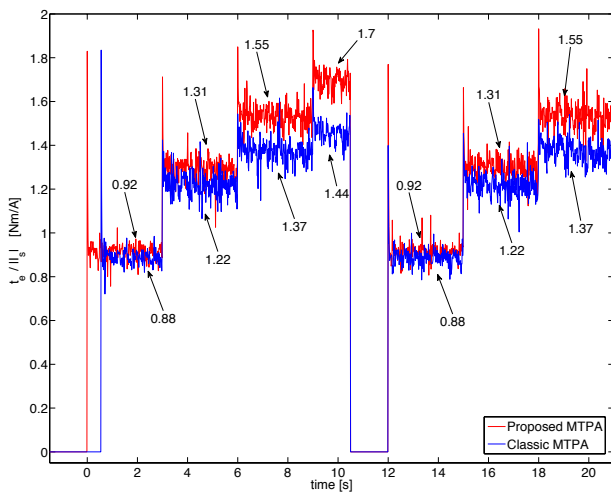


Fig. 9. *TPA* curve with the classic and the proposed *MTPA*

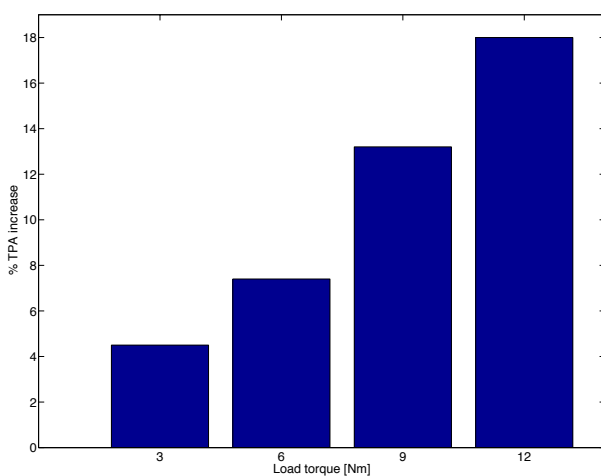


Fig. 10. *TPA* percent increase versus load achieved with the proposed *MTPA*

If the real *MTPA* is adopted, the rate of change of i_{sx} with i_{sy} is even lower than in the proposed *MTPA*. Fig. 8 shows the corresponding waveforms of the reference and measured speeds, obtained with the proposed *MTPA* and the classic one during the test. An instantaneous speed reduction is observable at each increase of the load torque, to which the control system reacts with a prompt dynamic increase of the electromagnetic torque. This is identically true for the proposed *MTPA* and the classic one, with negligible differences, as expected. It can thus be inferred that the adoption of the proposed *MTPA* in place of the classic one does not imply any difference in the dynamic behavior of the *SynRM* drive, as expected. Fig. 9 shows the instantaneous torque per ampere (*TPA*) curves as well as the average values of the *TPA* obtained for each value of the load torque.

In the computation of the $TPA = t_e / |I_s|$, the instantaneous value of the electromagnetic torque t_e should be used. The adopted experimental set-up, however, is not equipped with a torque-meter. The electromagnetic torque should consequently be estimated on-line on the basis of eq. (6). Such an estimation is potentially affected by several errors, mainly arising from the dependence of the static inductances on the two axis from the stator current components, see eq.s (2). On the contrary, the adopted experimental set-up is equipped with an industrial *PMSM* torque controlled drive, behaving as active load. Since the reference load torque t_L provided to the *PMSM* drive is a known quantity inside the control system, it has been used in Fig. 9 in place of the electromagnetic one. The load torque coincides with the electromagnetic one, $t_e = t_L$, at steady-state; during each stator current transient, occurring after the application of the step load torque, the measured stator currents are lower than their reference values, implying that the load torque is higher than the electromagnetic one. This account for the spikes of the *TPA* in Fig. 9 during the very first instants of each speed transient. For the above reasons, such spikes should not be considered since they are not part of the real physics of the system. The steady-state values of the *TPA*, on the contrary, almost constant during each speed transient, are to be considered reliable.

In Fig. 9, the instantaneous values of the *TPA* have been obtained with both the proposed *MTPA* and the classic one. It should be observed that the higher the load torque is, the higher the increment of the *TPA* achieved with the proposed *MTPA* with respect to the classic one is. This is to be expected, since for low loads the proposed *MTPA* trajectory coincides with that of the classic *MTPA*, whereas it deviates from it for high loads. In particular, for load torque equal to 12 Nm, the *TPA* obtained with the proposed *MTPA* is 1.7 against 1.44 obtained with the classic *MTPA*. Fig. 10 shows the steady-state percentage increase of the *TPA* obtained with the proposed *MTPA* with respect to the classic one versus the load torque. It can be noted that the adoption of the proposed *MTPA*, accounting for the magnetic saturation, permits a significant increase of the *TPA* in the whole load range, from 5% at 3 Nm load to 18% at 12 Nm load. Such results confirm the goodness of the proposed approach.

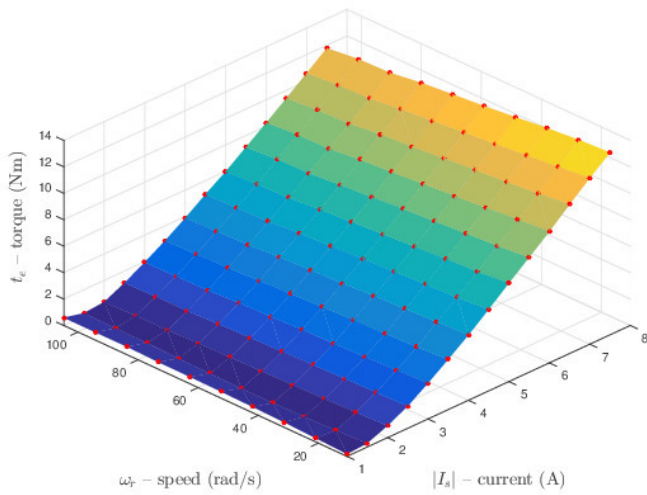


Fig. 11. Steady-state maximum producible torque vs rotor speed and stator current amplitude

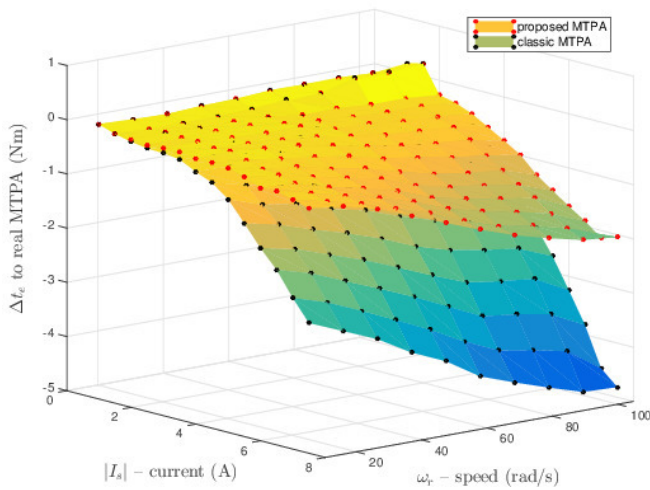


Fig. 12. Steady-state loss of maximum producible torque vs rotor speed and stator current amplitude

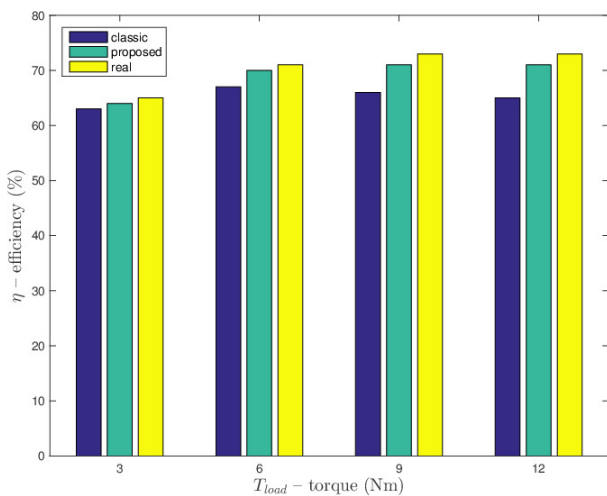


Fig. 13. Steady-state percent efficiency versus load torque at constant speed of 50 rad/s

B. Test 2: Steady-state test

This test presents the steady-state results, showing the electromagnetic torque which can be produced by the *SynRM* drive in the entire working range of stator current and rotor speed. This test has been performed three times, respectively with the proposed *MTPA*, with the classic *MTPA* and with the real *MTPA*. As for the real *MTPA*, the following procedure has been adopted for finding, in each working point, the real experimental *MTPA*. The *SynRM* drive, working with the rotor-oriented control in which the classic *MTPA* has been integrated (see Fig. 4), has been operated in current control (the speed control loop has been excluded). On the contrary, the *PMSM* drive exploited as active load has been operated in speed control; a specific constant rotor reference speed has been given to the *PMSM* drive (starting from zero reference speed). Then, as for the *SynRM* drive, the stator current amplitude $|i_s|$ is kept constant and, starting from the working condition at $\delta = \pi/4$ (classic *MTPA*), the angle δ has been spanned of a certain amount in both directions; this procedure has been carried on till the maximum electromagnetic torque is obtained. The torque angle δ_{max} and the corresponding maximum electromagnetic torque t_{emax} are then stored as real *MTPA* for the selected amount of stator current amplitude $|i_s|$ and speed ω_r . It should be noted that, for obvious reasons, such a method cannot be used on-line for controlling the optimal value of i_{sx} . Fig. 11 shows the experimental points (red) describing the relationship between the steady-state real maximum torque versus the stator current amplitude and the rotor speed, for the *SynRM* drive under test. The same graph shows also the corresponding interpolating surface. It can be observed that the maximum producible torque increases quickly with the stator current amplitude, while decreases slightly at for increasing values of the rotor speed, as expected, because of the presence of the iron losses increasing with the machine speed.

After having characterized the *SynRM* drive in terms of real *MTPA*, it has been operated in the same working points respectively with the proposed *MTPA* and with the classic one. The maximum values of the producible torque with both *MTPAs* have been stored for each value of rotor speed and stator current amplitude. As a result, Fig. 12 shows two surfaces describing the loss of maximum producible torque Δt_e versus the stator current amplitude $|i_s|$ and speed ω_r . Δt_e represents the difference between the real maximum torque and the maximum torque, obtainable respectively with the proposed *MTPA* and with the classic one. Fig. 12 shows, superimposed, the experimental points and the interpolating surfaces. It can be observed that, for all the values of the stator current amplitudes and rotor speeds, the loss of maximum producible torque with the proposed *MTPA* is much lower than that with the classic *MTPA*. In particular, the loss of maximum torque with the proposed *MTPA* is very small, lower or equal to 1 Nm (around 7 % of the rated torque), in almost the entire range of load torque and speed. Only for contemporary very high values of load torque and speed, basically close to the rated power of the motor, the loss of torque increases becoming about 14% of the rated torque. On the contrary, the loss of maximum torque with the classic *MTPA* is much higher than that with the proposed *MTPA* in the entire range of working load torque and speed,

becoming close to 36 % for very high values of the speed and torque, close to the rated power of the motor. Such results, in general, confirm the significant improvements achievable with the proposed *MTPA* with respect to the classic one. Furthermore, such results confirm that the proposed *MTPA* performs very closely to the real *MTPA* in almost the entire range of load and speed of the motor. The highest loss of torque observable with the proposed method can be explained considering that the variation of the stator inductance on the quadrature axis versus the corresponding current is not considered, while such variation becomes significant for very high values of the quadrature current. Finally, Fig. 13 shows the steady-state percent efficiency of the *SynRM* versus the load torque, obtained for the constant working speed of 50 rad/s. The graph has been obtained three times, with the classic *MTPA* (blue), with the proposed *MTPA* (green) and finally with the real *MTPA* (yellow). The real *MTPA* graph clearly shows a slight increase of the percent efficiency of the *SynRM* drive with the load, as expected, ranging between 65% and 75%. Moreover, the efficiency achieved with proposed *MTPA* is higher than that obtained with the classic *MTPA* and slightly lower than that obtained with the real *MTPA*, as expected. The higher the load is, the higher the difference between the efficiencies obtained respectively with the proposed *MTPA* and the classic one is.

VI. CONCLUSIONS

This paper presents an analytical formulation of a maximum torque per ampere (*MTPA*) technique, accounting for the magnetic saturation of the iron core, specifically developed for Synchronous Reluctance Motors (*SynRMs*). This technique is obtained with the development of a simplified magnetic saturation model of the *SynRM*, which has been derived from a more complete magnetic model including also cross saturation effects. The parameterization of the simplified magnetic model, and consequently of the proposed *MTPA*, can therefore be easily made by directly starting from a unique set of tests for the off-line identification of the motor, without the need for any complex, time consuming, and cumbersome finite element analysis (*FEA*) of the machine under test.

The proposed *MTPA* has been tested experimentally on a suitably developed test set-up. Results clearly show that the proposed technique permits a significant increase of the TPA with respect to the case of the classic *MTPA*, ranging from 5% at 3 Nm load to 18% at 12 Nm load. Moreover, the loss

of maximum torque, with respect to the real *MTPA*, obtained at the maximum speed and load torque with the proposed *MTPA* is about 15%, whereas the loss of maximum torque obtained with the classic *MTPA* is about 38.5%.

REFERENCES

- [1] P. Vas, *Sensorless Vector and Direct Torque Control*. Oxford Science, 1998.
- [2] L. Xu, X. Xu, T. A. Lipo, and D. W. Novotny, "Vector control of a synchronous reluctance motor including saturation and iron loss," *IEEE Trans. Ind. Appl.*, vol.27, no.5, pp.977–985, Sep./Oct. 1991.
- [3] R. E. Betz, R. Lagerquist, M. Jovanovic, T. J. E. Miller, and R. H. Middleton, "Control of synchronous reluctance machines," *IEEE Trans. Ind. Appl.*, vol.29, no.6, pp.1110–1122, Nov./Dec. 1993.
- [4] A. Vagati, M. Pastorelli, and G. Franceschini, "High performance control of synchronous reluctance motors," *IEEE Trans. Ind. Appl.*, vol.33, no. 4, pp. 983–991, Jul./Aug. 1997.
- [5] A. Vagati, M. Pastorelli, F. Scapino, G. Franceschini, "Impact of cross saturation in synchronous reluctance motors of the transverse-laminated type," *IEEE Trans. Ind. Appl.*, vol. 36, n. 4, Jul./Aug. 2000, pp. 1039–1046.
- [6] Y. Li, Z. Q. Zhu, D. Howe, and C. M. Bingham, "Modeling of cross-coupling magnetic saturation in signal-injection-based sensorless control of permanent-magnet brushless AC motors," *IEEE Trans. Magn.*, vol. 43, no. 6, Jun. 2007, pp. 2552–2554.
- [7] E. M. Rashad, T. S. Radwan, and M. A. Rahman, "A maximum torque per ampere vector control strategy for synchronous reluctance motors considering saturation and iron losses," in *Conf. Rec. IEEE IAS Annu. Meeting*, Oct. 2004, pp. 2411–2417.
- [8] Y. Inoue, S. Morimoto, and M. Sanada, "A Novel Control Scheme for Maximum Power Operation of Synchronous Reluctance Motors Including Maximum Torque Per Flux Control," *IEEE Trans. Ind. Appl.*, vol.47, no. 1, pp. 115–121, Jan./Feb. 2011.
- [9] J. Bonifacio, and R. M. Kennel, "On Considering Saturation and Cross-Coupling Effects for Copper Loss Minimization on Highly Anisotropic Synchronous Machines," *IEEE Trans. Ind. Appl.*, vol.54, no. 5, pp. 4177–4185, Sept./Oct. 2018.
- [10] H. A. A. Awan, Z. Song, S. E. Saarakkala, M. Hinkkanen, "Optimal Torque Control of Saturated Synchronous Motors: Plug-and-Play Method," *IEEE Trans. Ind. Appl.*, vol.54, no. 6, pp. 6110–6120, Nov./Dec. 2018.
- [11] H. W. de Kock, A. Rix, and M. J. Kamper, "Optimal torque control of synchronous machines based on finite-element analysis," *IEEE Trans. Ind. Electron.*, vol. 57, no. 1, pp. 413–419, Jan. 2010.
- [12] A. Accetta, M. Cirrincione, M. Pucci, A. Sferlazza, "A Saturation Model of the Synchronous Reluctance Motor and its Identification by Genetic Algorithms", *2018 IEEE Energy Conversion Congress and Exposition (ECCE)*, 2018, pp. 4460 – 4465.
- [13] A. Accetta, M. Cirrincione, M. C. Di Piazza, G. La Toma, M. Luna, M. Pucci, "Analytical Formulation of a Maximum Torque per Ampere (*MTPA*) Technique for *SynRMs* Considering the Magnetic Saturation", *IEEE Energy Conversion Congress and Expo 2019 (ECCE 19)*, 29 Sept. – 3 Oct. 2019, Baltimore, USA.